



Orbital Debris

Quarterly News

Volume 27, Issue 2
June 2023

Inside...

DAS Release..... 2

Recent Advances in
Modeling Hollow Objects
During Reentry..... 3

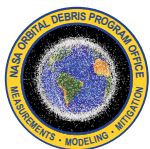
Two Years of Space Traffic:
Current Trends in
New Payloads and
Debris in Orbit..... 4

Overview of ORDEM Web
Application Features..... 6

Workshop Report..... 10

Upcoming Meetings..... 11

Space Missions and
Satellite Box Score..... 11-12



A publication of the
NASA Orbital Debris
Program Office (ODPO)

ISS Maneuvers Twice in a Week's Span to Avoid Potential Collisions

The International Space Station (ISS) performed a Predetermined Debris Avoidance Maneuver (PDAM) on 06 March 2023 at 12:42 GMT to avoid a projected high-risk conjunction with the NUSAT-17 MARY spacecraft. This vehicle (International Designator 2020-079J, U.S. Satellite Catalog Number 46835) is an Argentinean Earth observation spacecraft launched on 06 November 2020. The PDAM was executed using the 83P *Progress* vehicle's thrusters for a 0.7 m/s posigrade maneuver. The ISS apogee and perigee altitudes were raised by 1.14 km and 1.37 km, respectively.

A second PDAM was conducted on

14 March 2023 at 11:54 GMT to avoid a high-risk conjunction with Cosmos 1408 debris (1982-092PZ, Catalog Number 49982). This debris was created by the November 2021 anti-satellite test on Cosmos 1408 by the Russian Federation (ODQN vol. 26, issue 1, March 2022, pp. 1-5). The 83P *Progress* vehicle's thrusters were again used to perform a 0.3 m/s posigrade maneuver. ISS apogee and perigee altitudes were raised by 0.73 km and 0.40 km, respectively.

These events constitute the 34th and 35th collision avoidance maneuvers conducted by the ISS against tracked objects since 1999. ♦

Three Minor Breakups in First Quarter of 2023

The first breakup of calendar year 2023 occurred on 04 January 2023 at 03:57 GMT when the Cosmos 2499 spacecraft suffered its second known breakup event after more than 8 years on orbit, and 1.2 years after the 23 October 2021 event (ODQN vol. 26, issue 1, March 2022, p. 7). The vehicle (International Designator 2014-028E, U.S. Satellite Catalog Number 39765) had an orbital apogee and perigee altitude of 1537 km and 1163 km, respectively, with an inclination of 82.45°.

In addition to the parent body, 20 fragments (piece tags AD-AY, corresponding to Catalog Numbers 55717 to 55736) have entered the catalog. A Gabbard plot of this debris cloud is presented in the figure.

Readers are referred to a prior ODQN news article for a description of Cosmos 2491-class vehicles, of which Cosmos 2499 is a member (ODQN vol. 24, issue 1, February 2020, p. 3). As noted in that article, vehicles of this class, predicated upon their observed orbital behavior, likely feature multiple stored energy elements that may have initiated or contributed to the breakup process.

The second breakup of 2023 occurred on 10 February 2023 between 09:00 and 21:35 GMT, when the new Indian Small Satellite Launch Vehicle's (SSLV) SS3 solid fuel third stage fragmented after a 03:48 GMT launch from the Satish Dhawan Space Centre. The 2500 kg

continued on page 2

Three Minor Breakups

continued from page 1

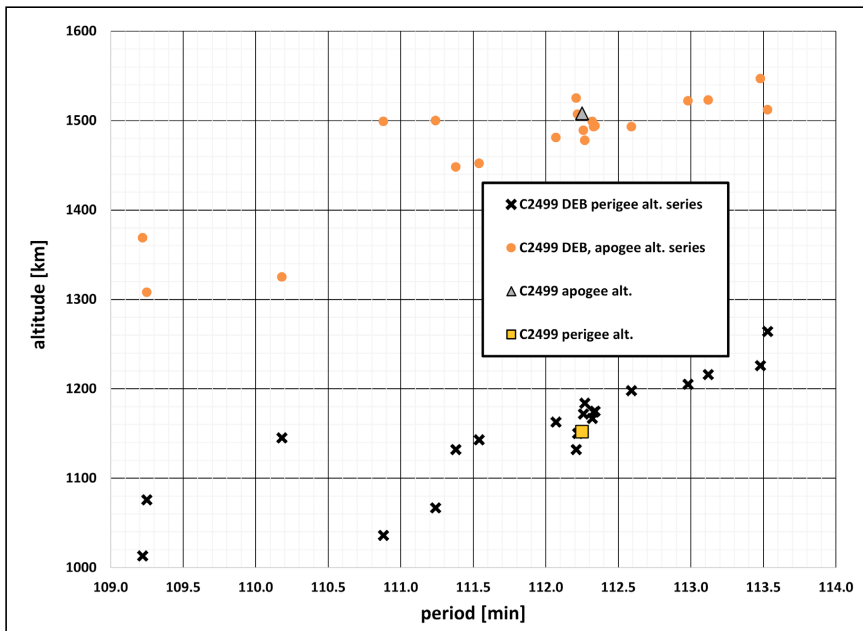


Figure. The Cosmos 2499 Gabbard plot. Epoch is approximately 20 March 2023. Maximum changes in orbital parameters are 3 minutes in period and 0.56° in inclination. This event is more energetic than the prior 23 October 2021 event.

dry mass (estimated) stage (2023-019D, Catalog Number 55565) was in a 442×357 km altitude, 37.2° inclination orbit when it broke up. This was the second launch of the SSLV. In addition to the SS3 parent body, five fragments (piece tags F-K, Catalog Numbers 55567, 55568, and 55737-9) were cataloged. All five breakup fragments reentered between 07 and 24 March 2023.

The third breakup of 2023 was that of the ORBCOMM FM 36 spacecraft (1999-065E, Catalog Number 25984), which broke up on 11 March 2023, 23.28 years after launch. This small, 45 kg communications spacecraft was the third of its kind to breakup, following FM 5 (ODQN vol. 26, issue 1, March 2022, p. 7) and FM 16 (ODQN vol. 23, issues 1 & 2, May 2019, pp. 1-2); readers are referred to the FM 16 article for a description of the vehicle and its inventory of stored energy. The spacecraft was in a 793×776 km altitude, 45.0° inclination orbit at the time of the event. As of 25 April 2023, no debris objects other than the parent body have entered the catalog. ♦

Debris Assessment Software 3.2.4 Release

The NASA Orbital Debris Program Office has released version 3.2.4 of the Debris Assessment Software (DAS), replacing the prior September 2022 release of DAS 3.2.3. The updated version provides data that can verify compliance of a spacecraft, upper stage, and/or payload with NASA's requirements for limiting debris generation, spacecraft vulnerability, post-mission disposal, and reentry safety.

This release incorporates updates to the user-defined material models for reentry calculations, a new automatic-upgrade feature for DAS project files for improved backwards compatibility, and a change to the solar flux table format.

Successful verification of a design in DAS demonstrates compliance with NASA orbital debris mitigation requirements. Historically, DAS analysis has proven acceptable in meeting the compliance requirements of agencies in the U.S. and around the world. It does not address the inherent design reliability facets of NASA requirements but addresses all Earth-related orbital debris requirements that make up the bulk of the requirements in the NASA Technical Standard 8719.14C. To calculate penetration risk from meteoroids, users should consult the NASA Meteoroid Environment Office and Hypervelocity Impact Technology teams for assessments.

For new users, DAS is available for download by permission only. An application must be completed via the NASA Software Catalog. To begin the process, click on the Request Software button in the catalog at <https://software.nasa.gov/software/MS-C-26690-1>.

Users who have completed the software request process for earlier versions of DAS 3.x do not need to reapply for DAS 3.2.4. Simply go to your existing account on the NASA Software Portal and download the latest installer. Due to file size limits, the installer has been split into several .zip archive files: the main installer and five separate files containing debris environment data. Users must download the main installer (which includes the debris environment for years 2016 to 2030) and additional environment files required to assess mission years beyond 2030.

Approval for DAS is on a per project basis: approval encompasses activities and personnel working within the project scope identified in the application.

PROJECT REVIEW

Recent Advances in Modeling Hollow Objects During Reentry

C. OSTROM, B. GREENE, AND J. MARICHALAR

Since 2018, the NASA Orbital Debris Program Office (ODPO) has undertaken a project to build and validate models for aerodynamic drag and aeroheating of hollow objects during atmospheric reentry [1, 2]. These efforts have been performed primarily in gas dynamic simulations of conditions relevant to reentry from low Earth orbit (LEO) using NASA's Direct Simulation Monte Carlo Analysis Code, or [DAC](#). The second phase of this project is ongoing, expanding the matrix of flow conditions and geometries from the previous 81 simulation cases to nearly 1000 and utilizing the results to reduce the uncertainty in the drag and heating coefficients used in the ODPO's Object Reentry Survival Analysis Tool (ORSAT) for the proposed hollow object model. The goal of this effort is to validate the current model assumptions, but also provide updates to the ORSAT drag and aeroheating models for an expanded set of reentering object shapes.

In parallel with the numerical simulations, the ODPO began a partnership with the University of Texas at San Antonio's (UTSA) Hypersonics Lab and conducted a test series using the on-site Mach 7 Wind Tunnel in October and November of 2022. The main purpose of this test series was to demonstrate that a Mach 7 wind tunnel could provide data sufficient to build and validate a drag and aeroheating model for implementation into ORSAT. This joint research project follows previous successful partnerships with the University of Texas at Austin (ODQN vol. 22, issue 3, p. 3, September 2018; ODQN vol. 23, issue 3, pp. 3-5, August 2019; and ODQN vol. 24, issue 2, pp. 5-6, April 2020).

A simple test matrix of 24 cases was designed to establish a performance baseline for the wind tunnel (see Table). Some of the test samples, made from aluminum and 3D-printed photopolymer, can be seen in Figure 1. All test cases were intended to run at a stagnation temperature of 700 K and a stagnation pressure of approximately 90 to 120 psi; the wind tunnel configuration [3] determined a test run time of around 0.1 seconds, sufficient to provide steady-state flow that could be compared with simulations using NASA's hypersonic computational fluid dynamics solver [Data Parallel Line Relaxation Code](#).

The test objects were released at the beginning of each run, allowing them to fly freely in the test section. The UTSA Hypersonics Lab developed a 3-D object tracking code incorporating multiple highspeed cameras. This new tracking code produces both

Table. List of geometric variables for wind tunnel test series.

Cross Section	Diameter or Width (inches)	Length (inches)	Inner Hole Size (inches)
Circle	0.5	0.125	0 (Solid)
Circle	0.5	0.125	0.05
Circle	0.5	0.125	0.25
Circle	0.5	0.125	0.45
Circle	0.5	0.5	0 (Solid)
Circle	0.5	0.5	0.05
Circle	0.5	0.5	0.25
Circle	0.5	0.5	0.45
Circle	0.5	1.5	0 (Solid)
Circle	0.5	1.5	0.05
Circle	0.5	1.5	0.25
Circle	0.5	1.5	0.45
Square	0.5	0.125	0 (Solid)
Square	0.5	0.125	0.05
Square	0.5	0.125	0.25
Square	0.5	0.125	0.45
Square	0.5	0.5	0 (Solid)
Square	0.5	0.5	0.05
Square	0.5	0.5	0.25
Square	0.5	0.5	0.45
Square	0.5	1.5	0 (Solid)
Square	0.5	1.5	0.05
Square	0.5	1.5	0.25
Square	0.5	1.5	0.45

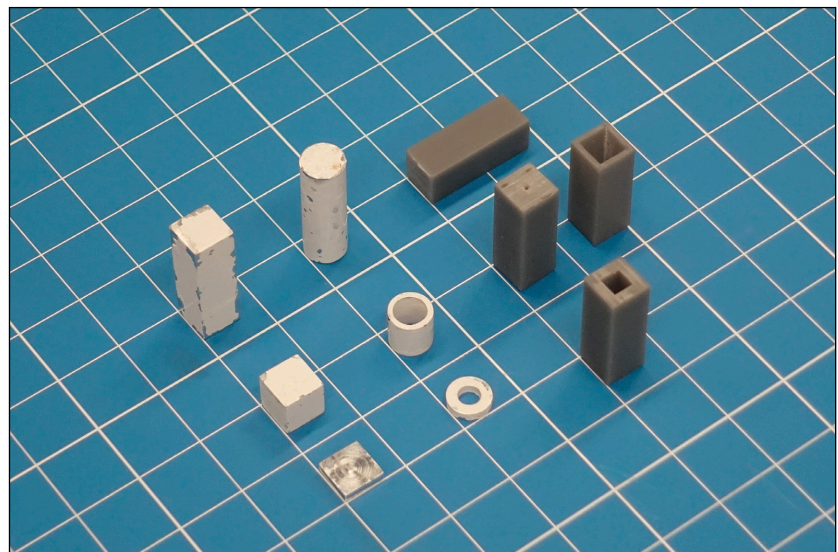


Figure 1. A selection of square and right circular cylinder wind tunnel test samples.

continued on page 4

Modeling Advances

continued from page 3

translational and rotational information for the object during the entire test or until the object moves beyond the visible part of the test section. A snapshot image of the tracking code's output can be seen in Figure 2, indicating the position and attitude of the object at this time stamp. Given the centroid coordinates and rotation angle of the object during a time series, the following parameters can be computed: drag, lift, and moment coefficients.

In addition to these kinetic measurements, temperature variations were analyzed using temperature sensitive paint (TSP) on 20 of the 24 test objects and high-speed infrared cameras for all 24 test objects, an example of which can be seen in Figure 3. TSP allows temperature measurements to be collected at the frame rate of the high-speed cameras. The lower frame-rate infrared camera measurements can be used to validate and calibrate the TSP. The measured temperature variations with time were used to compute heat flux over the visible surface of the test objects.

As a stretch goal for the test series, UTSA and the ODPO tested the performance of the wind tunnel using helium as the test gas rather than air. This change was expected to change the test section Mach number from approximately 7.0 to approximately 11.5 at the possible cost of degradation of the smoothness of the flow in the test section. While the tests at Mach 7.0 provided valuable validation data, a Mach number of 11.5 more closely matches the Mach number of reentering spacecraft at an altitude of between 60 km and 80 km, the altitude at which spacecraft typically encounter peak aerodynamic and heating effects. The two tests indicated that the Mach number indeed increased but only to approximately 11.0 due to unanticipated viscous effects. The flow in the test section also did not appear to be significantly degraded. These two test shots demonstrated additional capability at the UTSA Wind Tunnel facility to achieve flow conditions relevant to critical phases of atmospheric reentry.

Data processing is still underway to finalize the object tracking and TSP calibration. Once this data processing is complete, these tests will provide valuable validation data to compare to ORSAT hollow object drag models.

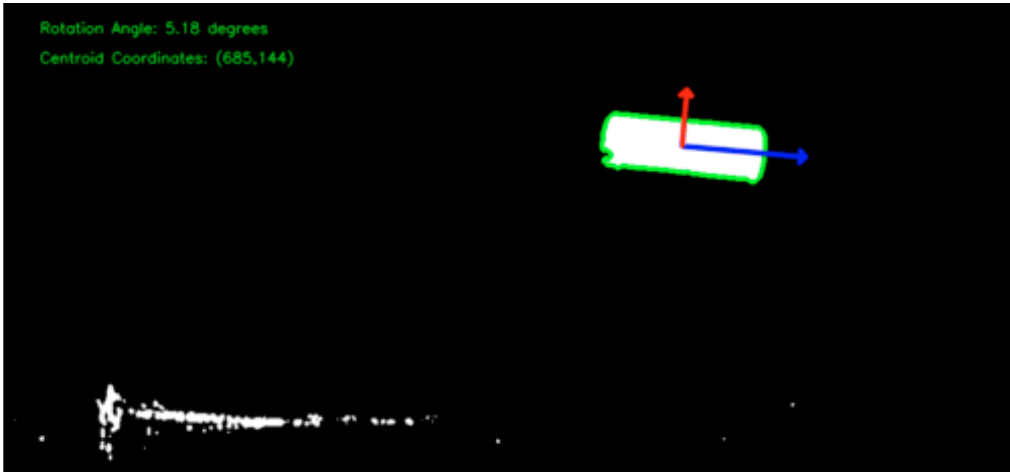


Figure 2. Snapshot of tracking code output for a 3 to 1 length-to-diameter cylinder.

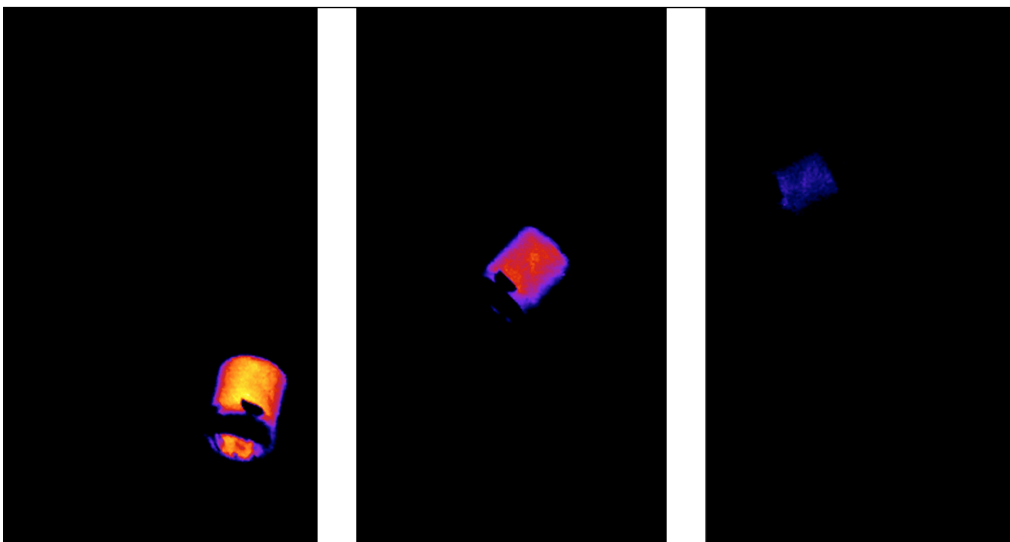


Figure 3. Three snapshots of a free-flying 1 to 1 length-to-diameter cylinder showing TSP fluorescence intensity, which is indirectly proportional to temperature.

References

1. Marichalar, J. and Ostrom, C. "Estimating Drag and Heating Coefficients for Hollow Reentry Objects in Transitional Flow Using DSMC [Direct Simulation Monte Carlo]," International Orbital Debris Conference, 2019.
2. Ostrom, C. "Challenges in Modeling Hollow Objects in the Transition Flow Regime," Aerothermodynamics and Design for Demise (ATD3) Workshop 2021.
3. Hoffman, E. *et al.* "Characterization of the UTSA Mach 7 Ludwig Tube," American Institute of Aeronautics and Astronautics SciTech Forum 2022. ♦

Two Years of Space Traffic: Current Trends in New Payloads and Debris in Orbit

B. GREENE

The NASA Orbital Debris Program Office (ODPO) maintains an internal database based on information available in the U.S. Satellite Catalog to define the historical, current, and predictions of the future state of the objects in Earth orbit. Each satellite is assigned an object type (spacecraft, upper stage, or debris), size, and wet and dry mass, if known, which are used within models of the orbital evolution of objects to assess orbit lifetime, the likelihood of collisions and explosions, and to estimate how they may influence the orbital debris environment directly or indirectly, singly or in aggregate.

Over the past two years, an average of 975 new tracked objects have been added to the catalog each quarter. New objects are added to the catalog when they are initially released on independent orbits, whether by a launch vehicle, a parent spacecraft during normal operation, or an anomalous event or breakup event. Independent objects temporarily attached to another object and released again later, such as a Dragon spacecraft docked to the ISS or a *Shenzhou* spacecraft docked to the *Tiangong* space station, are only counted once and do not get a new designation upon re-release. An analysis of the number and mass of different classes of objects illustrates trends in the space industry and the orbital population. Knowledge of these trends in how the space environment is being used can help inform space policy.

Figure 1 compares broad categories of new objects added to the catalog from the second quarter (Q2) of calendar year (CY) 2021 to Q1 CY2023. Over a third of all new objects came from the fragmentation of existing satellites (37.8% total). Mission-related debris (MRD), or inert objects released by a satellite during normal operation, accounted for 4.4% of all new objects. The majority of these are payload encapsulation or attachment hardware released during spacecraft deployment. Spent rocket bodies and orbit insertion motors accounted for 2.8% of new objects. The remaining 55.1% of objects that added to the space traffic from Q2 CY2021 through Q1 CY2023 are spacecraft.

Some trends are also evident in a quarter-by-quarter look at relative numbers of objects in four main categories. Figure 2 shows the number of new objects each quarter in the debris, large constellation (over 100 satellites), small constellation/single satellite payloads, and rocket bodies' category. Over the past two years, the launch cadence has increased. It should be noted that the number of rocket bodies in the catalog do not represent all launches, as many larger rocket upper stages perform a targeted de-orbit burn at end of mission and are never tracked for more than one or two rotations. The launch cadence also shows a periodicity, with fewer launches in the first quarter and a slow ramp-up over the course of the year.

The number of debris objects added to the catalog at any given time is largely driven by a background rate of

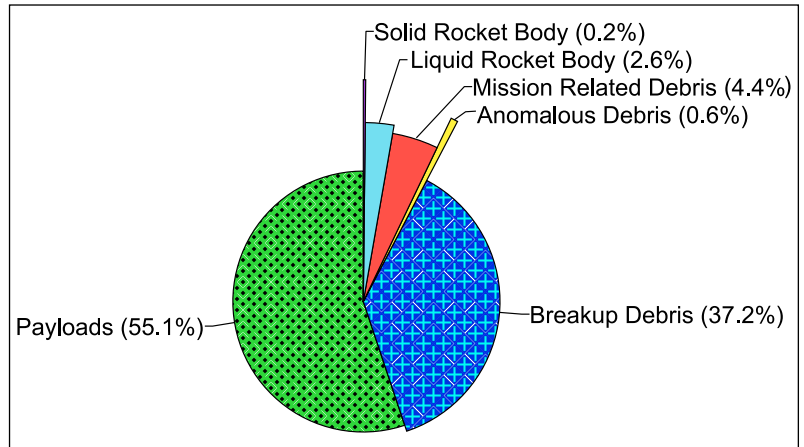


Figure 1. Pie diagram of object categories for all tracked objects added to the catalog since Q2 CY2021.

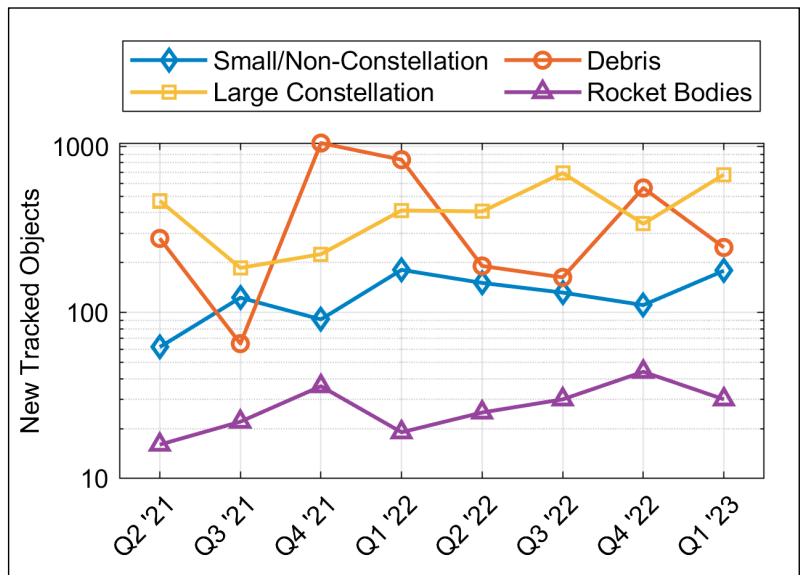


Figure 2. Small/non-constellation, large constellation, debris, and rocket body counts by quarter.

MRD production and discrete breakup events. Generally, the background rate of MRD production is 40 to 80 objects per quarter with another 50 to 100 objects added every quarter from old breakup events and small anomalous events. In Figure 2, two peaks in debris object creation correlate to two large breakup events: the Russian anti-satellite (ASAT) test on *Cosmos 1408* on 15 November 2021 and the breakup of a *Long March 6A* upper stage on 13 November 2022.

Large constellation launches have placed a relatively steady number of objects into orbit for most of the last two years and comprise more than half of all payloads launched. A short, two-quarter lull in large constellation payloads occurred in the final two quarters of 2021, during which several legal stays on further Starlink launches were requested.

continued on page 6

Space Traffic Trends

continued from page 5

Table. Mass range definitions for spacecraft size categories

Category	Mass Range
Femtosat	< 1 kg
Picosat	1 – 10 kg
Nanosat	10 – 50 kg
Microsat	50 – 100 kg
Minisat	100 – 300 kg
Medium Sat	300 kg – 1 ton
Large Sat	1 ton – 5 ton
Very Large Sat	> 5 ton

Breaking down the payloads by size and membership in a large constellation highlights some of the reasons that payload launches have increased. The satellite community uses various categories for different masses of satellites, and these may vary in definition depending on source. For purposes of this analysis, the categories of satellites as a function of mass are defined in the Table.

Figure 3 shows the category breakdown of all payloads for the last two years, and clearly indicates the recent trend towards large constellations and small payloads; nearly three quarters of all payloads are members of a large constellation and over half of the remaining payloads have a mass of less than 100 kg each. Nearly 8% of all payloads are CubeSats with dry masses under 15 kg. Less than 7% of payloads did not have sufficient information for classification, thus marked as uncategorized in Figure 3.

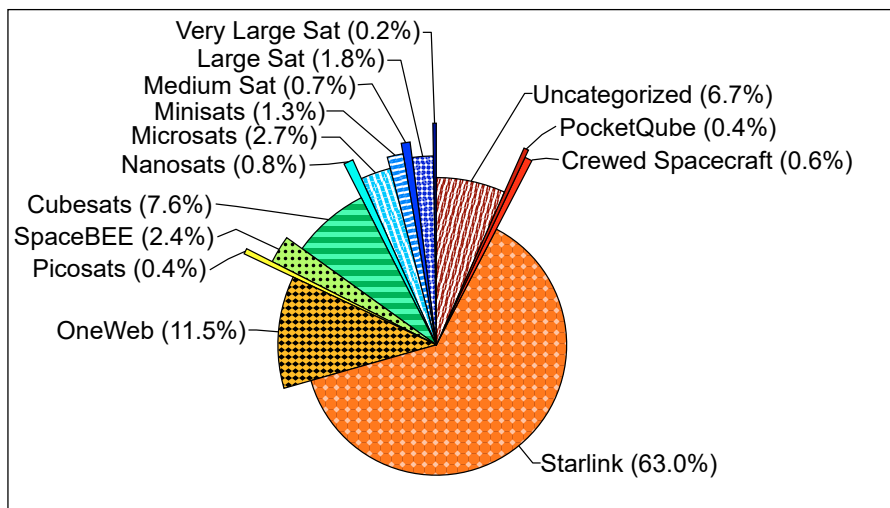


Figure 3. Pie diagram of payload categories for all payloads added to the catalog from Q2 2021 to Q1 2023.

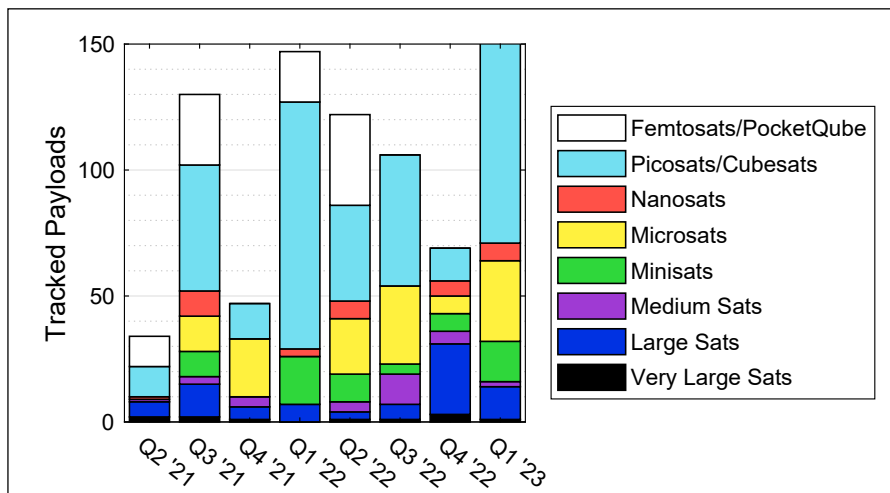


Figure 4. Payload categories by quarter, excluding the large constellation spacecraft: SpaceBEE, Starlink, and OneWeb.

The number of small constellations (with fewer than 100 members, such as FLOCK, LEMUR, and GlobalHawk) and single-satellite payloads launched has also increased since 2021, as shown in the total objects for each quarter in Figure 4. This increase is mostly driven by ride-share launches, dedicated multiple deployment missions like SpaceX’s “Transporter” launches, a burgeoning launch market for dedicated sub-100 kg payloads, and technology advances that allow more functionality in smaller, lower-mass packages. With the exception of Q4 2022, the overall trend in launching massive (payloads > 5 tons) is minimal; less than 15 payloads over the course of two years have exceeded this metric with Q4 2022 accounting for 3. This is in contrast to the number of small satellites (< 0.5 ton) that, on average has risen over the past two years. Satellites smaller than 30 kg (Picosats and smaller) make up more than half of these smaller payloads almost every quarter, and even smaller form-factor satellites are becoming popular, with more than half of all PocketQube spacecraft (Femtosats) ever launched making it to orbit in 2022.

Monitoring the historical space traffic environment allows the ODPO to project future space traffic and statistically assess a realistic space debris environment attributable to explosions and collisions. This provides the ODPO with the tools it needs to develop models that can be used to understand mission risk and evaluate realistic and actionable mitigation options. Additionally, monitoring space traffic can identify important trends in the space industry and the influence of these trends on the environment. ♦

Overview of the ORDEM Web Application Features

A. VAVRIN

The NASA Orbital Debris Program Office’s (ODPO) Orbital Debris Engineering Model (ORDEM) is widely used by mission designers and operators (NASA, U.S. government, industry, and the international community) for orbital debris impact risk assessments. To better serve the user community and support NASA Headquarters’ Digital Transformation Initiative, ORDEM is now available as a cloud-based web application, unveiled in ODQN, vol. 26, issue 2, p. 1. The ORDEM web application includes the current features of the publicly released ORDEM software (version 3.2) with an upgraded, frontend design. The underlying ORDEM mathematical model is the same as the standalone ORDEM 3.2, but instead of running these computations on a user’s workstation, it runs on a cloud container. This allows the user to run multiple spacecraft and telescope/radar mode simulations in parallel from the web browser of their choice in a cloud-based environment, thus minimizing any user specific computer limitations.

A brief workflow for completing an ORDEM run is as follows. After logging in with the proper credentials, the user is directed to the home page of the ORDEM web application, shown in Figure 1. The user can select one of the assessment modes from the top menu and can complete the form by entering the orbital elements (for Spacecraft mode) or sensor geometries (for Telescope/Radar mode) of their asset. The user can enter multiple orbit simulations or sensor geometries to the assessment. Upon completion, the user sends their assessment to the cloud, and the ORDEM backend interface will generate a unique job identification (job-id) for these tasks. This newly created 36-character job-id will be displayed on screen, and the user will be redirected to the Job Status page (also accessible from the top menu). The user can download the results after the job completes.

The assessment modes have a common page and button layout with the same fields as the standalone frontend option, as well as new options exclusive to the ORDEM web app. For spacecraft assessments, as shown in Figure 2, each set of orbital elements is assigned an auto-generated number once added to the task table. For telescope/radar assessments, as shown in Figure 3, sensor geometries are used instead of orbital elements. For both assessments, the

continued on page 8

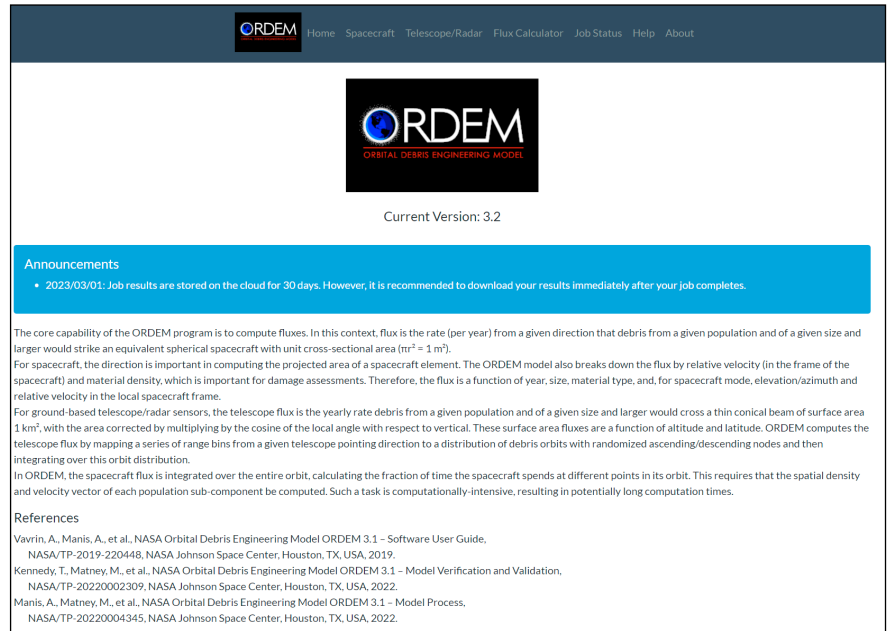


Figure 1. ORDEM web app home page.

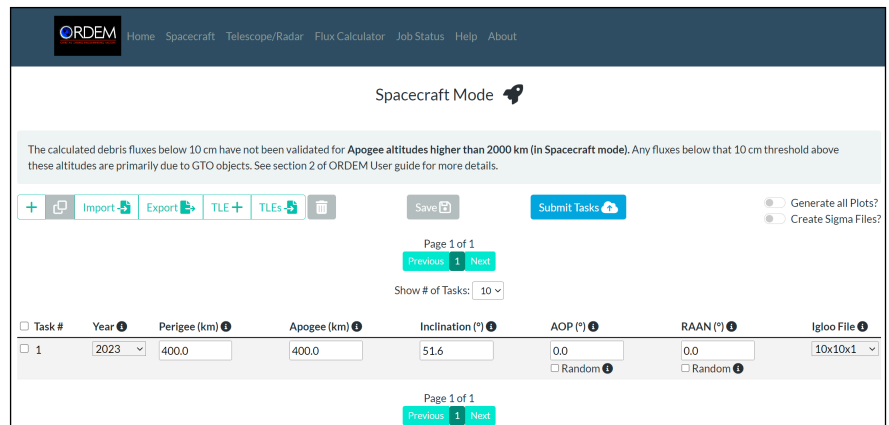


Figure 2. Spacecraft mode page.

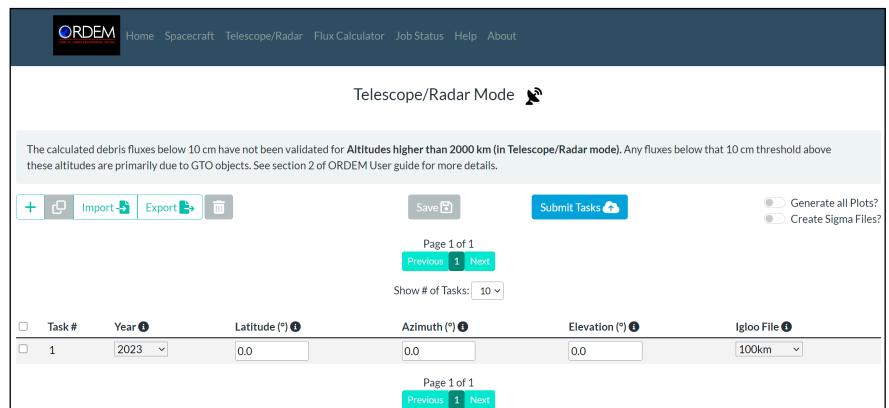



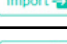




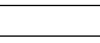


Figure 3. Telescope/Radar mode page.

ORDEM Overview

continued from page 7

Table. Spacecraft/Telescope Mode data entry options

Add		Adds a task of default values
Copy		Copies selected tasks
Delete		Deletes selected tasks
Import		Import tasks from .csv
Export		Export task table to .csv
Add TLE		Add task using a TLE dataset (Spacecraft-only)
Import TLEs		Import tasks from a file of TLE sets (Spacecraft-only)
Save		Saves tasks to the browser session
Submit		Submits all tasks to the cloud

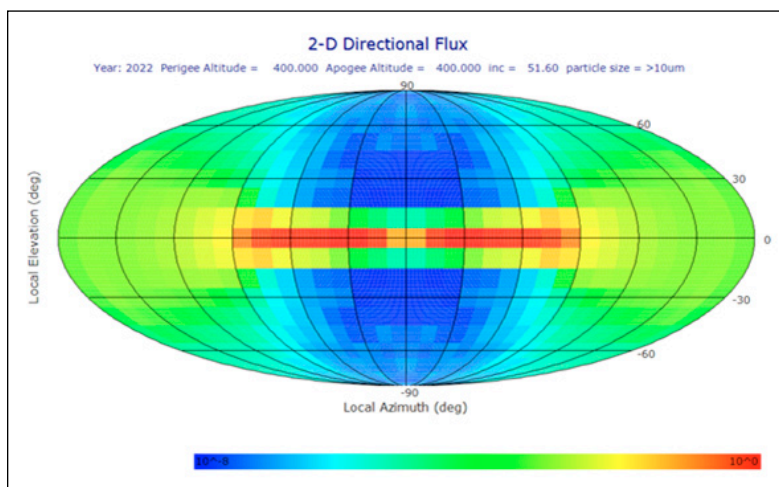


Figure 4. 2-D Directional Flux, 400 km x 400 km altitude, 51.6-degree inclination orbit, as produced by standalone ORDEM 3.2 frontend.

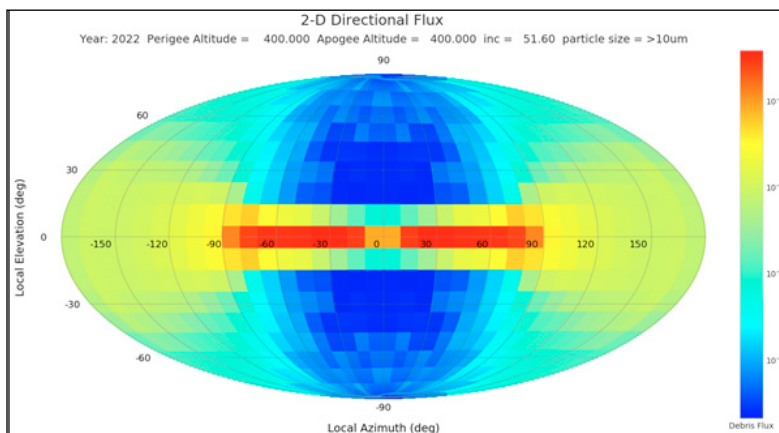


Figure 5. 2-D Directional Flux, 400 km x 400 km altitude, 51.6-degree inclination orbit, as produced by ORDEM web application.

input field validation rules from the publicly released ORDEM software are applied. Additional options for entering data in the assessment modes are described in the Table.

Two additional options are presented to the user shown in both Figure 2 and 3 as on or off slider buttons. The first option, "Generate all Plots?", will generate the standard plots for all tasks if checked (default is unchecked). These plots (*i.e.*, Average Flux versus Size, Velocity Flux, 2-D Directional Flux) are saved as high-resolution PNG files for each task. Figure 4 is an example of the 2-D directional flux plot (particle size > 10 μ m) for a 400 km x 400 km altitude, 51.6-degree inclination orbit from the standalone ORDEM 3.2 frontend, and Figure 5 is the same plot produced from the ORDEM web application. The second option, "Create Sigma Files?", will generate the igloo flux uncertainty files for all tasks if checked. However, if the user does not need the uncertainty files in their assessment, then leaving this option unchecked will speed up the ORDEM run and decrease the file size of downloaded results. For more information on the uncertainty files or different types of ORDEM plots, see the latest version of the [ORDEM Software User Guide](#). Note that there are no major changes between the ORDEM 3.1 and ORDEM 3.2 user guides. The plotting options and uncertainty calculations remain the same in both documents.

The Job Status page, accessible from the top menu, shows the progress of a submitted job. Once the user enters a valid job-id in the text field and clicks the Search button, the current progress for each task will display on the page. The status table includes several columns. The Folder Name column shows the unique folder names for each task. The Description column lists the orbital elements (spacecraft mode) or sensor targets (telescope/radar mode) for each task. The Phase column lists the orbit regions that are assessed in each task, and the overall phase will update as the ORDEM model continues running. The Progress column shows the percent completed for each phase. The Complete column shows a download link for each completed task. Once all tasks are complete, the user can download all tasks in a single compressed file by clicking the "ALL tasks (.zip)" button at the top of the status table. Figure 6 shows an example of a completed job with results ready for download to a user's local machine.

The ORDEM web application also includes a Flux Calculator for spacecraft assessments, as shown in Figure 7. Once the user uploads the necessary SIZEFLUX_SC.OUT file, an average flux is calculated based on the debris size entered in the text field. The level of uncertainty ("Sigma σ Factor") can be adjusted up to 3.0- σ , and the Upper Bound and Lower Bound fields

continued on page 9

ORDEM Overview

continued from page 8

are re-calculated each time Sigma factor is updated. The Decadal Points table shows the average flux at several standard ORDEM decadal size points. These table values are updated every time the user selects a valid Size Flux file.

For a better experience, the user should consider a few points. First, the maximum number of tasks per job is set to 150 to ensure a stable cloud experience; however, the goal is to remove this maximum limit soon. Next, users should also note that the cloud platform is designed to store the results of a user's job for a maximum of 30 days. Afterwards, the user will no longer be able to access their results, though jobs can be rerun if desired.

The ORDEM web application can be accessed at <https://ordem.appdat.jsc.nasa.gov/>. NASA users can access the ORDEM web application with Launchpad credentials. Non-NASA users can request access by creating an account at <https://guest.nasa.gov/>. The model is also available as stand-alone, downloadable packages from the NASA Software Catalog via <https://software.nasa.gov/software/MSC-25457-1>.

Reference

Vavrin, A., Manis, A., *et al.*, NASA Orbital Debris Engineering Model ORDEM 3.1 – Software User Guide, NASA/TP-2019-220448, NASA Johnson Space Center, Houston, TX, USA, 2019. ♦

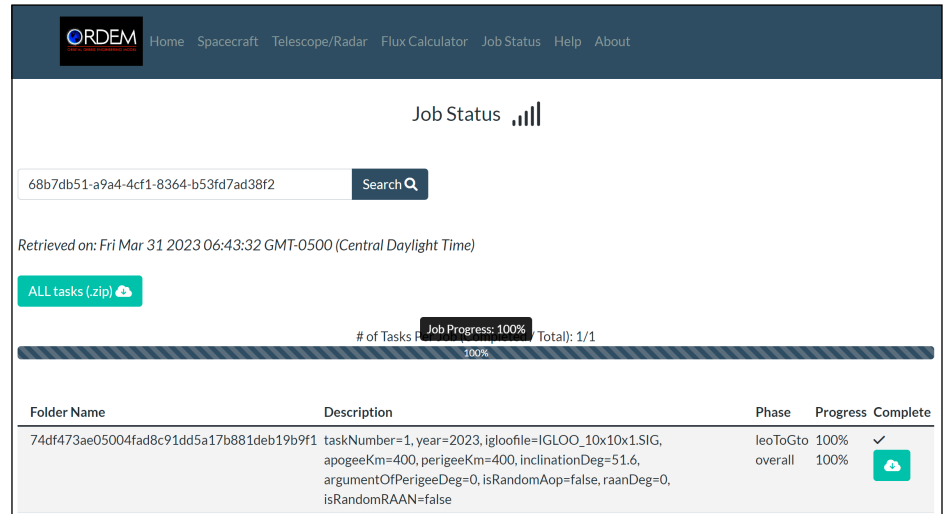


Figure 6. Job Status page, with a job ready for download.

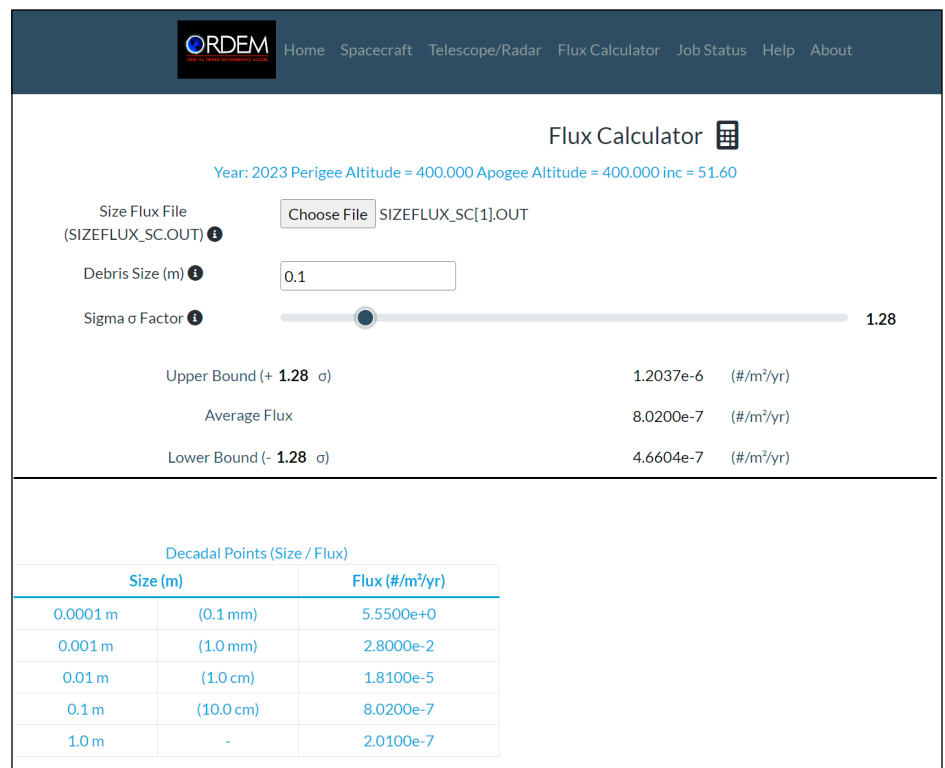


Figure 7. Flux calculator page.

The [NASA Orbital Debris Photo Gallery](#) has high resolution, computer-generated images of objects in Earth orbit that are currently being tracked. Photos and graphics may be freely downloaded from the NASA ODPO webpages, unless they include a third-party credit line. In these cases, permission must be granted by the copyright owner.

WORKSHOP REPORT

The Spacecraft Anomalies and Failures (SCAF) Workshop, 29-30 March 2023

The annual two-day Spacecraft Anomalies and Failures (SCAF) workshop was held 29-30 March 2023. The NASA Engineering and Safety Center hosted the unclassified Day 1 session at the NASA Goddard Space Flight Center, and the National Reconnaissance Office hosted the Day 2 classified sessions in Chantilly, Virginia. There were over 225 registered participants and 9 invited presentations for Day 1 and over 140 registered participants and 10 invited presentations for Day 2. A diverse group of U.S. and international aerospace community members were in attendance, including representatives from academia, industry, civil, and military space organizations. Focused on space environment interactions and anomaly resolution lessons learned, this workshop provided a chance for personnel from

a broad range of space-related areas to exchange concepts to improve space systems, such as anomaly and failure attribution tools and root-cause analysis practices.

Day 1 topics included discussions of the space environment, especially recent solar activity. There were also presentations on lessons learned from several high-profile NASA missions, such as the Double Asteroid Redirection Test (DART) spacecraft, the James Webb Space Telescope, and crewed human vehicles. In addition, presenters discussed the recurring theme of the importance of collaboration, sharing of information, and communication between space entities to achieve maximum mission success and space safety. The agenda for this workshop can be found here: <https://www.nasa.gov/nase/conferences/SCAF2023>. ♦

SUBSCRIBE to the ODQN or UPDATE YOUR SUBSCRIPTION ADDRESS

To be notified when a new issue of the ODQN is published or to update your email address, [subscribe](#) on the NASA Orbital Debris Program Office (ODPO) website at: <https://orbitaldebris.jsc.nasa.gov/quarterly-news/>

UPCOMING MEETINGS

05-10 August 2023: 37th Small Satellite Conference, Logan, Utah, USA

Utah State University (USU) and the American Institute of Aeronautics and Astronautics (AIAA) will sponsor the 37th Annual USU/AIAA Conference on Small Satellites under the theme “Missions Small at Satellite Scale.” This conference will explore future missions and delve into key technology drivers, operational constructs, and activities that inform and secure success of small satellite missions at scale. The call for abstracts ended on 02 February 2023. Registration is now open for attendees at <https://smallsat.org/>.

19-22 September 2023: 24th Advanced Maui Optical and Space Surveillance Technologies Conference (AMOS), Maui, Hawaii, USA

The technical program of the 24th Advanced Maui Optical and Space Surveillance Technologies Conference (AMOS) will focus on subjects that are mission critical to space situational awareness. The technical sessions include papers and posters on orbital debris; space situational/space domain awareness; adaptive optics and imaging; astrodynamics; non-resolved object characterization; and related topics. The abstract submission deadline was 01 March 2023. Registration for this hybrid conference is now open for in-person and virtual attendees. Additional information about the conference is available at <https://amostech.com>.

02-06 October 2023: 74th International Astronautical Congress (IAC), Baku, Azerbaijan

The IAC will convene in 2023 with a theme of “Global Challenges and Opportunities: Give Space a Chance.” Of note, the 24th IAC was last held in Baku 50 years ago in 1973. The IAC’s 21st International Academy of Astronautics Symposium on Space Debris will cover debris measurements and characterization; modeling; risk analysis; hypervelocity impact and protection; mitigation; post-mission disposal; space debris mitigation and removal; operations in the space debris environment; political and legal aspects of mitigation and removal; orbit determination and propagation; and financial gains with space debris. This year, the IAC will offer a venue for interactive presentations on space debris topics to allow more digital display capabilities for attendees. The abstract submission deadline passed on 28 February 2023. Information about the conference and registration is available at <https://www.iafastro.org/events/iac/iac-2023/> and <http://iac2023.org/>. ♦



2ND INTERNATIONAL ORBITAL DEBRIS CONFERENCE

DECEMBER 4–7, 2023
HOUSTON, TEXAS AREA

The 2nd International Orbital Debris Conference (IOC) will convene December 4–7, 2023. The conference goal is to highlight orbital debris research activities in the United States and to foster collaborations with the international community. The four-day, in-person conference will cover all aspects of micrometeoroid and orbital debris research, operations and

mission support, environment management, and other related activities. The deadline for the submission of abstracts closed on April 6, 2023, after an extension. The final program for IOC II will be released in June 2023. More information is available at <https://www.hou.usra.edu/meetings/orbitaldebris2023/>. ♦

INTERNATIONAL SPACE MISSIONS
01 January 2023 – 31 March 2023

Intl.*Designator	Spacecraft	Country/Organization	Perigee Alt. (KM)	Apogee Alt. (KM)	Incl. (DEG)	Addnl. SC	Earth Orbital R/B	Other Cat. Debris
1998-067	ISS dispensed objects	Various	412	419	51.6	3	0	1
2022-144E	USA 340	US	35915	35948	3.0	0	0	0
2022-144F	USA 341	US	NO ELEMS AVAILABLE					
2022-144G	LINUSS1	US	36086	36177	2.6			
2022-144H	LINUSS2	US	36090	36175	2.6			
2023-001B	MENUT	SPN	518	532	97.5	98	0	0
2023-002A	SJ-23	PRC	35737	35745	0.8	0	2	0
2023-003A	OBJECT A	PRC	518	525	97.3	4	0	0
2023-004A	ONEWEB-0532	UK	752	755	86.8	39	0	0
2023-005A	APSTAR 6E	PRC	EN ROUTE TO GEO			0	2	0
2023-006A	SHIYAN 22A (SY-22A)	PRC	489	508	43.2	0	1	0
2023-006B	SHIYAN 22B (SY-22B)	PRC	500	516	43.2			
2023-006C	YAOGAN-37	PRC	506	519	43.2			
2023-007A	OBJECT A	PRC	492	514	97.4	13	0	0
2023-008A	USA 342	US	35343	35369	0.0	0	1	2
2023-008B	LDPE-3A	US	35971	35977	0.2			
2023-009A	NAVSTAR 82 (USA 343)	US	20168	20197	55.1	0	0	0
2023-010A	STARLINK-5277	US	567	572	70.0	50	0	4
2023-011A	HAWK-6B	US	543	548	40.5	0	2	0
2023-011C	HAWK-6C	US	543	548	40.5	548	40.5	
2023-011D	HAWK-6A	US	544	547	40.5			
2023-012A	IGS R-7	JPN	NO ELEMS AVAILABLE			0	1	0
2023-013A	STARLINK-5492	US	558	560	43.0	55	0	4
2023-014A	STARLINK-5077	US	357	361	70.0	48	0	5
2023-014BC	ION SCV-009	IT	387	396	70.0			
2023-014BH	EBAD TEST MASS	IT	271	276	70.0			

continued on page 12

SATELLITE BOX SCORE

(as of 03 May 2023, cataloged by the
U.S. SPACE SURVEILLANCE NETWORK)

Country/ Organization	Spacecraft*	Spent Rocket Bodies & Other Cataloged Debris	Total
CHINA	609	4357	4966
CIS	1567	5734	7301
ESA	96	29	125
FRANCE	86	538	624
INDIA	113	105	218
JAPAN	204	108	312
UK	673	1	674
USA	6047	5115	11162
OTHER	1181	85	1266
Total	10576	16072	26648

* active and defunct

Visit the NASA

Orbital Debris Program Office Website

www.orbitaldebris.jsc.nasa.gov

Technical Editor

Heather Cowardin, Ph.D.

Managing Editor

Ashley Johnson

Correspondence can be sent to:

Robert Margetta

robert.j.margetta@nasa.gov

or to:

Shaneequa Vereen

shaneequa.y.vereen@nasa.gov

National Aeronautics and Space Administration
Lyndon B. Johnson Space Center
2101 NASA Parkway
Houston, TX 77058



www.nasa.gov

<https://orbitaldebris.jsc.nasa.gov/>

INTERNATIONAL SPACE MISSIONS

01 January 2023 – 31 March 2023

Intl.* Designator	Spacecraft	Country/ Organization	Perigee Alt. (KM)	Apogee Alt.(KM)	Incl. (DEG)	Addnl. SC	Earth Orbital R/B	Other Cat. Debris
2023-015A	STARLINK-5699	US	552	555	43.0	52	0	4
2023-016A	ELEKTRO-L 4	CIS	35778	35796	0.4	0	1	0
2023-017A	AMAZONAS 6	BRAZ	EN ROUTE TO GEO			0	1	0
2023-018A	PROGRESS MS-22	CIS	412	419	51.6	0	1	0
2023-019A	EOS-7	IND	431	438	37.2	0	2	5
2023-019B	AZAADISAT-2	IND	407	431	37.2			
2023-019C	JANUS-1	US	373	401	37.2			
2023-020A	STARLINK-5749	US	558	560	43.0	54	0	4
2023-021A	STARLINK-5484	US	567	572	70.0	50	0	4
2023-022A	INMARSAT 6-F2	IM	EN ROUTE TO GEO			0	1	0
2023-023A	CHINASAT-26	PRC	35771	35802	0.1	0	1	0
2023-024A	SOYUZ MS-23	CIS	412	419	51.6	0	1	0
2023-025A	HORUS 1	EGYP	486	506	97.5	0	1	2
2023-026A	STARLINK-30050	US	355	355	43.0	20	0	0
2023-027A	DRAGON ENDEAVOUR 4	US	412	419	51.6	0	0	0
2023-028A	STARLINK-5592	US	533	538	70.0	50	0	4
2023-029A	ONEWEB-0530	UK	591	593	86.5	39	0	0
2023-030A	OBJECT A	PRC	891	892	99.0	0		
2023-030B	OBJECT B	PRC	878	884	99.0			
2023-030C	OBJECT C	PRC	759	883	99.0			
2023-030D	OBJECT D	PRC	891	892	99.0			
2023-031A	LUCH (OLYMP) 2	CIS	35784	35789	0.1	0	1	1
2023-032A	HORUS 2	EGYP	490	501	97.5	0	1	4
2023-033A	DRAGON CRS-27	US	260	409	51.6	0	0	1
2023-034A	SHIYAN 19 (SY-19)	PRC	492	514	97.5	0	0	0
2023-035B	CAPELLA-10 (WHITNEY)	US	590	595	44.0	0	2	0
2023-035C	CAPELLA-9 (WHITNEY)	US	591	596	44.0			
2023-036A	GAOFEN 13 02	PRC	35777	35795	3.0	0	1	0
2023-037A	STARLINK-5856	US	428	432	70.0	51	0	4
2023-038A	SES 18	SES	35706	35784	0.1	0	1	0
2023-038B	SES 19	SES	35784	35787	0.0			
2023-039A	OBJECT A	PRC	499	522	97.4	0	1	0
2023-039B	OBJECT B	PRC	499	519	97.4			
2023-039C	OBJECT C	PRC	499	516	97.4			
2023-039D	OBJECT D	PRC	498	514	97.4			
2023-040A	COSMOS 2567	CIS	494	507	97.6	0	1	0
2023-041B	GLOBAL-19	US	443	452	42.0	0	2	1
2023-041C	GLOBAL-5	US	440	451	42.0			
2023-042A	STARLINK-5905	US	419	421	43.0	55	0	4
2023-043A	ONEWEB-0537	UK	552	575	87.1	35	1	0
2023-044A	OBJECT A	ISRA	NO ELEMS AVAILABLE			0	0	0
2023-044B	OBJECT B	ISRA	NO ELEMS AVAILABLE					
2023-045A	COSMOS 2568	CIS	320	337	96.5	0	1	0
2023-046A	STARLINK-6102	US	433	435	43.0	55	0	4
2023-047A	OBJECT A	PRC	507	524	97.4	0	0	0
2023-047B	OBJECT B	PRC	509	527	97.4			
2023-047C	OBJECT C	PRC	507	527	97.4			
2023-047D	OBJECT D	PRC	514	529	97.4			
2023-048A	OBJECT A	PRC	1082	1098	63.4	0	0	0
2023-048B	OBJECT B	PRC	913	1097	63.4			

Intl. = International; SC = Spacecraft; Alt. = Altitude; Incl. = Inclination; Addnl. = Additional; R/B = Rocket Bodies; Cat. = Cataloged

Notes: 1. Orbital elements are as of data cut-off date 31 March. 2. Additional spacecraft on a single launch may have different orbital elements. 3. Additional uncataloged objects may be associated with a single launch.